Urban Heat Island Effect based on Temporal Analysis of Land Surface Temperature for Rawalpindi and Islamabad

By

Syeda Nageen Fatima Zaidi

216/FBAS/MSES/F14

Department of Environmental Sciences

Faculty of Basic and Applied Sciences

International Islamic University Islamabad

(2017)

Urban Heat Island Effect based on Temporal Analysis of Land Surface Temperature for Rawalpindi and Islamabad

Researcher:
Syeda Nageen Fatima Zaidi
216/FBAS/MSES/F14

Supervisor:
Dr. Syeda Maria Ali
Assistant Professor

Department of Environmental Sciences

Faculty of Basic and Applied Sciences
International Islamic University Islamabad

(2017)

بسم الله الرحمن الرحيم

Department of Environmental Science

International Islamic University Islamabad

Dated: 11-01-2017

FINAL APPROVAL

It is certificate that we have read the thesis titled as "Urban Heat Island Effect Based on Temporal Analysis of Land Surface Temperature for Rawalpindi and Islamabad" submitted by Syeda Nageen Fatima and it is our judgment that this project is of sufficient standard to warrant its acceptance by the International Islamic University, Islamabad for the M.S Degree in Environmental Sciences.

COMMITTEE

External Examiner

Dr. Azra Yasmin
Professsor,
Department of Environmental Science,
Fatima Jinnah Women University, Rawalpindi

Internal Examiner

Dr. Zafeer Saqib
Assistant Professor,
Department of Environmental Sciences,
International Islamic University, Islamabad

Supervisor

Dr. Syeda Maria Ali
Assistant Professor,
Department of Environmental Sciences,
International Islamic University, Islamabad

Dean, FBAS

International Islamic University, Islamabad

A thesis submitted to Department of Environmental Sciences, International Islamic University, Islamabad as a partial fulfillment of requirement for the award of the degree of MS Environmental Science

DEDICATION

This project is dedicated to all environmentalists who are making efforts to save communities from natural disasters by making the ecosystems resilient.

Syeda Nageen Fatima Zaidi

DECLARATION

I hereby declare that the work presented in this report is my own effort, except where otherwise acknowledged and that the report is my own composition. No part of this project report has been previously presented for any other degree.

Date 6-02-2017

Syeda Nageen Fatima Zaidi

Table of Contents

ACKNOWLEDGEMENTS

First of all I am grateful to the ALMIGHTY ALLAH for His blessings and making me able to complete this study. I wish to express my sincere gratitude to my supervisor Dr. Syeda Maria Ali. I am extremely grateful and indebted to her for her expert, sincere and valuable guidance and encouragement extended to me throughout the course of this study. I also place on record my sense of gratitude to Chairperson, DES for her support. I also like to thank Mr. Junaid Aziz Khan and Mr Iftikhar Ali Mashwani for their guidance. I would like to acknowledge Pakistan Metrological Department (PMD) for providing necessary data. I will also express my thanks and love to my friends Komal Haroon, Aneeza Islam, Saba Iqbal, Shehzadi Saba and Irum Rahim for their endless support and wishes during my study. In the end, I would like to extend thanks to my family for their love and support.

Syeda Nageen Fatima Zaidi

LIST OF ABBREVIATIONS

Acronym	Abbreviation
UHI	Urban Heat Island
DN	Digital Number
TM	Thematic Mapper
ERDAS	Earth Resources Data Analysis System
ETM	Enhanced Thematic Mapper
GIS	Geographic Information System
LST	Land Surface Temperature
LULC	Land use and Land Cover Change
MSS	Multi Spectral Sensor
NDVI	Normalized Difference Vegetation Index
NIR	Near Infra Red
IR	Infra Red
OLI	Operational Land Imager
TIRS	Thermal Infra Red Sensor
ENVI	Environmental Visualization
PMD	Pakistan Metrological Department

LIST OF FIGURES

LIST OF TABLES

Table No. **Page No.**

Abstract

Urbanization is amongst one of the most concerned environmental issue associated with Urban Heat Island (UHI) effect is the most alarming. This study has been conducted to identify emergence of UHI in Rawalpindi and Islamabad in last two decades i.e. from 1993 to 2015. Landsat TM, ETM+ and OLI-TIRS were used to generate the land use land cover (LULC) patterns, land surface temperature and UHI intensity zones in addition to ground stations data. Massive urbanization has changed the natural LULC of study area with a significant increase in built up area and a decrease of vegetation and forest. This anthropogenic interference has resulted in high temperature zones modifying the climate of urban areas producing UHI effect.

Chapter 1

INTRODUCTION

1.0 Introduction

Climate change is a global phenomenon but the contributing and underlying causes of climate change occur locally and regionally gradually affecting the globe's climate (Seinfeld and Pandis, 2016). Urbanization is significantly gaining momentum around the world as a result of development, population growth and shifts and expansion of commercial and residential centers. Formation of these urban agglomerations is often unplanned and changes the natural landscape (Coseo and Larsen, 2014). According to UN (World Urbanization Prospects 2010), more than half of world's population resides in urban areas and the projected urban population in 2050 is 69.6%. As a result of this urban sprawl, many environmental issues arise including deforestation, excessive consumption of water and energy resources and congestion. These issues intensify and pose a combined effect to increase the overall temperature of urban areas (Huang *et al.*, 2015) Scientists have observed that the temperature in densely built and populated areas is higher than the surrounding rural areas. This effect is known as "Urban Heat Island" (Coseo and Larsen, 2014).

The term "urban heat" was first used by Luke Howards in early 1800s when he found significantly high temperature in London city as compared to its village areas (Gartland, 2012). For years, the reason for high urban temperature was unclear. A lot of research was conducted on UHI in the past decades. After vigorous observation and investigation it was found that UHI is formed in metropolitan areas that are relatively warmer due to anthropogenic activities such as towns and mega cities (Voogt, 2007; Sidiqui *et al.*, 2016). Temperature records have been greatly influenced by expansion of urban centers during 20th and 21st centuries (Balogun *et al.*, 2011). The annual mean temperature of the city with more than 1 million people can be 1-3°C higher than its rural surroundings. In the evening, the temperature difference is as high as 12 °C because the heat absorbed in the day is emitted back into the atmosphere by urban surfaces (USEPA). A study conducted in 2014 involved 65 states in United States and Canada and indicates that the densely populated urban areas are experiencing the UHI effect every summer The study stated that forests areas have clearly cooler temperature then the built up areas (Zhao *et al.*, 2014). Isotherm of UHI is shown as a flattened curve at the sides representing rural surroundings and a rising curve in the center representing the urban areas. The temperature difference can be clearly spotted through the difference in both curves (Gago *et al.*, 2013).

1.1 Primary Triggering factors behind UHI Phenomenon

Introduction of urban materials and human modification in landscape has caused implications for urban environments (Hanqiu and Benqing, 2004). Urban sprawl occurs both vertically and horizontally resulting in blockage of air due to congested and tall buildings and preventing ventilation (Mizaei, 2015).Vehicular emissions, emissions from power plants and air conditioners and heat absorbed in urban structures results in formation of UHI (Memon *et al.*, 2009). Primary factors behind UHI phenomenon include:

- Low albedo characteristics of Urban Materials e.g. asphalt, concrete, glass and steel which have more heat absorbing and less heat reflecting potential.
- Inadequacy of natural evaporative surfaces e.g vegetation and moist soil to provide a balanced heat mechanism.
- High production of pollutants that meddle with the natural radiative characteristics of the earth.
- Heat produced through anthropogenic activities.
- Vertical buildings that supplements heat absorption by providing more surface area and blocking the urban ventilation that could lower the temperature otherwise.

1.2 Interrelation of Land Surface Temperature (LST) with Land Use and Land Cover (LULC)

High temperature is the distinct characteristic of urban areas as compared to rural areas (Schwarz *et al.*, 2012). Transformation of natural landscape into anthropogenic land use and land cover is an obvious aspect of urbanization because it requires the provision of infrastructure, energy and other amenities for the growing population (Shudo *et al.*, 1997). The forests and grasslands are transformed into impervious surfaces causing the earth's physical properties to change and this change affects UHI (Lo and Quattrochi, 2003). The formation of big cities affects the quality of environment often causing pollution, traffic congestion and elevated energy budget (Mirzae, 2015). The roads, buildings and other infrastructure absorb heat and keep the temperature high even after the sunset (Xian and Crane, 2006). Moreover, increased population in cities, a greater number of transportation vehicles and lots of anthropogenic activities produces more heat. On the other hand rural areas cool down quickly as there is less infrastructure and dense vegetation which helps in maintaining lower temperatures. The empirical studies of temperature data show that the climate of cities significantly differs from the rural areas (Li *et al.*, 2015).

The main reason for high LST in cities is human disturbances and modified landscape in cities. (Dikhan *et al.*, 2015) evaluated temporal UHI effect along the coastal zone of Istanbul for 1984-2011 using Landsat TM and ETM+ images. The results of their study show that the existence of UHI is closely related to LULC and LST patterns. The impervious class of the LULC drastically changes the LST and has a significant role in formation of UHI (Su *et al.*, 2010). Urban surfaces are mainly made from concrete, glass, steel, stone or asphalt which have excellent insulating and heat holding capacity. For example, water in a lake and a concrete roof will have different absorption capacities. The urban surfaces have very high absorption potential and low albedo as compared to natural surfaces such as trees and water resulting in high temperatures during day and night (Brazel *et al.*, 2000). Moreover, urban surfaces and towns are paved decreasing the amount of soil moisture thus changing the amount solar radiation is absorbed on earth.

LST is closely related to land use and land cover of any area and acts as a standard for urban climate (Gusso *et al.*, 2015; Munier and Burger, 2001). Thus the assessment of UHI should involve detailed analysis of LST of urban areas. (Sheng *et al.*, 2015) mapped the UHI in Hangzhou, China by analyzing the LST. They found that the proportion of impermeable surfaces and vegetation cover has a major role in UHI formation. Vegetation provides a medium for evapo-transpiration so land with green cover loses heat quickly (Bass *et al.*, 2002). Eumorfopoulou and kontoleon, 2009) performed an experimental study on two buildings by covering one building with plants and keeping the other one bare and compared the thermal behavior of both. The results showed clear temperature difference with lower temperature on the plant covered wall. (Upmanis *et al.*, 1998) and (Upmanis, 1999) carried out a study to evaluate the urban climate near parks. Their study indicates that the parks play a significant role in minimizing temperature of the surroundings. (Zhang *et al.*, 2013) deduced that deforestation and loss of water bodies has created a major contribution towards the existence of UHI. (Kumar *et al.*, 2012) found that the maximum air temperature was present in the built up areas and minimum temperature was observed in densely vegetated areas. Vigorous research repeatedly reports that the UHI effect is observed over built up area or the open land with heat holding soil characteristics (Pena, 2008).

1.3 Approaches to Study UHI

To offset the undesirable phenomenon of UHI and neutralizing the urban temperatures, many policies and strategies have been devised and numerous researches have been conducted using different approaches and methods. Empirical evidence from the literature shows that observations of ground based temperature stations and the satellite based Land Surface Temperature (LST) data are mainly used for detection of UHI (Hamdi, 2010). A study was conducted to estimate the urban heat island in Mumbai city, India. Land use and land cover classes and LST was used to inspect the cause of rising temperature. It was found that the highest temperatures were in built up areas of the city. The study showed a directly proportional relationship between LST and built up index where as the vegetation index and LST showed opposite relationship (Dwivedi *et al.*, 2015). (Liu and Zhang, 2011) analyzed the effect of UHI in Hong Kong based on vegetation and built up analysis and LST and suggested the remote sensing and GIS as a convenient tool for conducting climate related researches.

The advent of GIS and remote sensing based tools and techniques has provided advantageous opportunity for detailed studies of earth's landscape and its thermal characteristics in less time with high accuracy and low cost (Rawat and Kumar, 2015; Balogun *et al.*, 2011; Aniello *et al.*, 1995). Various researches show that remotely sensed data is significantly useful in analysis of UHI effect and its relation to land use and land cover (Kandel *et al.*, 2016; Huang *et al.*, 2015; Quan *et al.*, 2014; Gago *et al.*, 2013; Kumar *et al.*, 2012; Liu and Zhang, 2011; Imhoff *et al.*, 2010). For greater reliability of results, the climatic data from ground based stations and accuracy assessment should be integrated with the satellite data processing (More *et al.*, 2015; Dwivedi *et al.*, 2015). (Huang *et al.*, 2015) utilized Landsat TM and ETM+ images to analyze the thermal characteristics of urban expansion in Changsha, China. They delineated urban and sub-urban areas and their expansion density and examined the patterns of LST and UHI intensity. They concluded that the urban sprawl and its thermal characteristics can be analyzed though satellite data. (Weng *et al.*, 2004) performed a remote sensing based investigation on urban clusters in Zhujiang Delta, China and found vegetation as an influential factor in mitigation of high LST. Satellite based data is convenient for the study of UHI phenomenon due to its global coverage and continuous provision of data. In contrast, Ground stations based data does not provide the data for every point on ground and involves high cost and maintenance (Yusuf *et al.*, 2014).

1.4 Implications of UHI

High temperature in urban areas affects the life quality and ecosystem functioning often triggering heat waves during summers. 800 people died in Chicago heat wave in 1995 (Changnon *et al.*, 1996). Excessive deaths were reported during heat wave in UK in August 2003 (Wright *et al.*, 2005). There are a number of negative impacts on health and environment due to UHI that include elevated energy demand in which high temperatures during summer increase the demand for cooling (Schwarz *et al.*, 2012). So increased energy demand puts pressure on resources and causes load shedding and shortages of power. As UHI increases the energy demand, greenhouse gases are emitted from power plants and electric appliances. Power plants which rely on fossil fuels for energy production emit sulfur dioxide, nitrogen dioxide, carbon monoxide and particulate matter which pollute the air, and helps in the formation of smog. These power plants also produce carbon dioxide which is a major climate change instigator (Voogt, 2007).

High temperature and air pollution linked with UHI cause many health implications for humans and biodiversity including general discomfort, heat strokes, breathing difficulties, heat cramps and heat related mortality (Schwarz *et al.*, 2012). UHI give rise to extreme and abnormal hot weather condition known as heat wave. Children, older individuals and patients are most likely to be affected by such events and the mortality rate can reach above average (Wright *et al.*, 2005). Center for disease control and prevention declared that the heat exposure has caused 8,000 pre-mature deaths in United States from 1979-2003 (Knowlton *et al.*, 2009). Roads, pavements and rooftops having high temperature can heat the storm water impairing its quality. When this water runs off in streams, rivers and ponds, it proves threatening to the aquatic life and hinders their metabolism and reproduction sometimes causing death of organisms (Zhao *et al.*, 2014).

Pakistan is no exception to the effects of urbanization and climate change. The country has a population of 180 million people and the urban population has been projected to be 60% in 2050 by United Nations Department of Economic and Social Affairs (UDESA, World Population Prospects, 2011). Different studies indicate that Pakistan has faced massive urbanization during last 20 years (Sajjad *et al.*, 2015). 2000 people were killed in Karachi heat wave during June, 2015 as temperature level reached above 50°C (Salim *et al.*, 2015). There is a need to formulate strategies to counteract this warming but the identification and mapping of UHI is the prerequisite for that.

Table 1.1: Various studies in comparison with current study

S.No	Study Area	Title of the Research	Author and Year
1	Rawalpindi and Islamabad (Current Study)	Urban Heat Island Effect based on Temporal Analysis of Land Surface Temperature for Rawalpindi Islamabad	
2	Sydney, Australia	Spatio-temporal mapping and monitoring of urban heat island over Sydney, Australia using Landsat 8 and MODIS	(Sidiqui *et al.*, 2016)
3	South Florida, USA	An analysis on the UHI effect using radiosonde profiles and Landsat imagery with ground meteorological data in South Florida.	(Kandel *et al.*, 2016)
4	Tehran, Iran	Seasonal variation of the surface urban heat island in a semi arid city.	(Haashemi *et al.*, 2016)
5	Lahore, Pakistan	Mapping urban heat island effect in comparison with land use and land cover of Lahore district.	(Shah and Ghauri, 2015)
6	Mumbai, India	Estimation of Land Surface Temperature to study Urban Heat Island effect in Mumbai using Landsat ETM+ Image.	(Dwivedi *et al.*, 2015)
7	Changsha, China	An analysis of urban expansion and its thermal characteristics using Landsat Imagery.	(Huang *et al.*, 2015)
8	Istanbul, Turkey	Evaluation of Surface urban heat island effect on coastal zone of Istanbul Megacity.	(Dikhan *et al.*, 2015)
9	Hangzhou, China	Impacts of land cover types on urban heat island in	(Sheng *et al.*, 2015)

		Hangzhou, China.	
10	India	Study of different approaches used to estimate the UHI effect in India	(More *et al.*, 2015)
11	USA and Canada	Strong contributions of local background climate to urban heat islands.	(Zhao *et al.*, 2014)
12	Kuala Lumpur, Malaysia	Spatio-temporal assessment of urban heat island effects in Kuala Lumpur metropolitan city using Landsat.	(Yusuf *et al.*, 2014)
13	Chicago, USA	How factors of land use/land cover, building configuration and adjacent heat sources and sinks explain UHI in Chicago.	(Coseo and Larsen, 2014)
14	Beijing, China	Multi-temporal trajectory of UHI centroid in Beijing, China	(Quan *et al.*, 2013)
15	Shanghai, China	Analysis of land use/land cover change, population shift, and their effects on the spatio-temporal patterns of UHI in metropolitan Shanghai, China.	(Zhang *et al.*, 2013)
16		The city and urban heat islands: A review of strategies to mitigate adverse effects.	(Gago *et al.*, 2013)
17	Leipzig, Germany	Relationship of land surface and air temperatures and its implications for quantifying UHI indicators. An application for the city of Leipzig.	(Schwarz *et al.*, 2012)
18	Vijayawada, Andhra Pradesh, India	Estimation of land surface temperature to study urban heat island effect using Landsat ETM+	(Kumar *et al.*, 2012)
19	Hong Kong, China	Urban heat island analysis using the Landsat TM and Aster data. A case study in Hong Kong.	(Liu and Zhang, 2011)
20	Akure, Nigeria	Analysis of urban expansion and land use changes in Akure, Nigeria using remote sensing and GIS techniques	(Balogun *et al.*, 2011)
21	Uccle, Brussels, Belgium	Estimating UHI effects on the temperature series of Uccle (Brussels, Belgium) using remote sensing data and a land surface scheme.	(Hamdi, 2010)
22	Nanjing City, China	Assessing the effect of land use and land cover on urban heat island pattern in Nanjing City, China	(Su *et al.*, 2010)
23	Biomes of Continental USA	Remote sensing of urban heat island effects across biomes in the continental USA.	(Imhoff *et al.*, 2010)
24	Northern Greece	Experimental approach to the contribution of plant covered walls to the thermal behavior of building envelopes.	(Eumorfopoulou and Kontoleon, 2009)
25	Santiago, Chile	Relationship between remotely sensed surface parameters associated with the urban sink formation in Santiago, Chile.	(Pena, 2008)
26	Greece	Daytime urban heat islands from Landsat ETM+ and corine land cover data: An application to major cities in Greece.	(Stathopoulou and Cartalis, 2007)
27	Tampa Bay and Las Vegas, USA	An analysis of urban thermal characteristics and associated land cover in Tampa Bay and Las Vegas using Landsat satellite data	(Xian and Crane, 2006)
28	Seoul, Korea	Spatial and temporal structure of the urban heat island in Seoul.	(Kim and Baik, 2005)
29	Manchester and London, UK	Dwelling temperatures and comfort during the August 2003 heat wave.	(Wright *et al.*, 2005)
30	Zhujiang Delta,	Estimation of land surface temperature-vegetation	(Weng, 2004)

	China	abundance relationship for UHI studies	
31	Xiamen City, China	Remote sensing of the urban heat island and its changes in Xiamen City of SE China.	(Hanqiu and Benqing, 2004)
32	Atlanta, USA	Land use and land cover change, urban heat island phenomenon and health implications.	(Lo and Quattrochi, 2003)
33	Beijing, China	Detecting and analyzing urban heat island patterns in Beijing, China	(Xiao *et al.*, 2002)
34	Berlin, Germany	Analysis of land use data and surface temperatures derived from satellite data for the area of Berlin.	(Munier and Burger, 2001)
35	Baltimore and Phoenix, USA	The tale of two climates: Baltimore and Phoenix urban LTER sites.	(Brazel *et al.*, 2000)
36	Goteborg, Sweden	The influence of sky-view factor and land use on city temperatures: Influence of parks on local climate	(Upmanis, 1999)
37	Goteborg, Sweden	The influence of green areas on nocturnal temperatures in a high latitude city.	(Upmanis *et al.*, 1998
38	Hokkaido, Japan	A study on temperature distribution influenced by various land uses.	(Shudo *et al.*, 1997)
39	Chicago, USA	Impacts and responses to the 1995 heat wave: A call to action.	(Changnon *et al.*, 1996)
40	Dallas, Texas, USA	Mapping micro urban heat island using Landsat TM and GIS.	(Aniello *et al.*, 1995)

1.5 Significance of the Study

To curb global climate change, UHI mapping should be done for urban environments. Urban Heat Island seems to be a local phenomenon but in turn it contributes to global warming, so reducing the causes of UHI will help meet the global climatic challenges. Identification of urban heat hotspots is the basic step for the implementation of mitigation strategies. This research will provide information to the urban planners and climate change specialists to study urban climatic conditions and devise resilience strategies for the cities.

1.6 Objectives

1. To estimate the land use and land cover changes of Rawalpindi and Islamabad from 1993 to 2015.
2. To study the temperature changes during the past 2 decades by temporal analysis of Land surface Temperature (LST).
3. Identification of Urban Heat Islands in Rawalpindi and Islamabad.

Chapter 2

Materials and Methods

2.0 Materials and Methods

This chapter includes the description of materials, tools and methods used to achieve the objectives of this study. The datasets, softwares and procedures used to detect and map the urban heat island hotspots have been described in detail.

2.1 Study Area

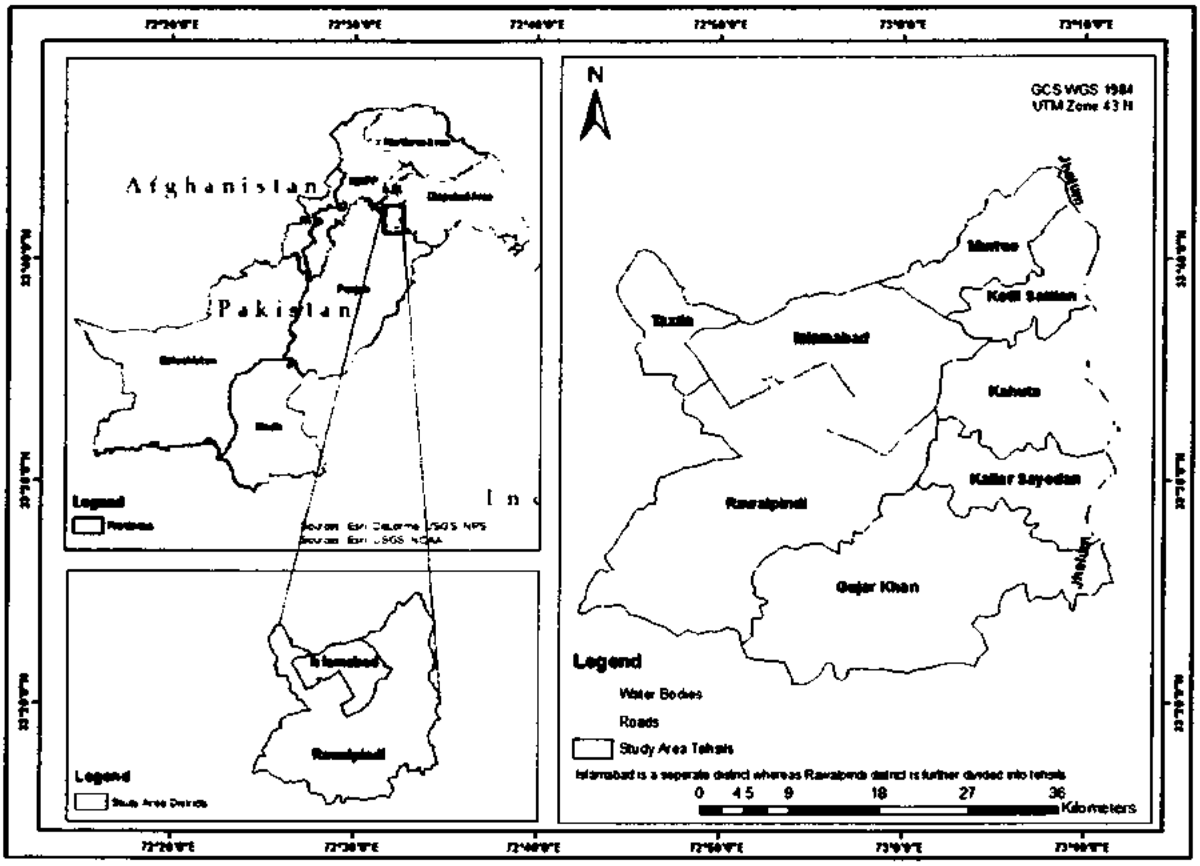

Figure 2.1: Study Area Map

2.1.1 Location and Extent

The study area comprises of district Rawalpindi and Islamabad that lies between 34.08°N 73.63°E and 72.62°S 33.06°W. It constitutes a total area of 6114 square km together and the third largest metropolitan area of Pakistan. Islamabad is the capital of Pakistan and a major hub for all business centers, government institutions, embassies and consulates. It is a planned city constructed in 1960's and experienced massive urbanization and extension with big shopping malls, commercial and residential estates and sectors still under-construction. Rawalpindi district on the other side is comprised of 7 tehsils including the old colonial Rawalpindi city, the ancient Taxilla, Kahuta, Gujar khan, Kallar Syedan, Kotli Sattian and a relatively cool hill station known as Murree at an elevation of 2,291 m. Among these areas, Islamabad and Rawalpindi city are highly urbanized and others are advancing rapidly as new urban centers develop and rural areas are being transformed into towns (Shiekh *et al.*, 2007).

2.1.2 Demography

According to 1998 Census, the total population of study area was 4.1 million comprising of 51.20% males and 48.80% females. Most of the population was residing in urban areas with population density of 765/Sq Km. The population was projected to rise at an annual average growth rate of 3.97%. Literacy rate is 70% and significant portion of population is educated (Pakistan Bureau of Statistics, 1998).

2.1.3 Climate

The climate of study area varies due to different geographical attributes and altitude of different tehsils. The climate of Islamabad and Rawalpindi city is hot and humid in summers with temperatures reaching to 45°C and cold in winters with temperature falling below 0°C. The hottest month is June and the coldest months are December and January. July and August are the monsoon seasons when the area experiences significant rainfall. The average annual rainfall is 1200 mm and average humidity is 55%. Murree hill station is an exception with pleasant and cool summers where average temperature is 25°C and relatively colder winters where average temperature falls below -4°C. High rainfall sometimes exceeds the monthly average of 2000 mm and precipitation occurs in the form of snow during winter (Sheikh *et al.*, 2007; Un-Habitat, 2014).

2.1.4 Geology

The study area consists of alluvial plains and hilly terrain with Margalla and Murree hills spreading towards western Himalayas. Consolidated rocks in the area are almost 50 million years old and composed of Surghar group, Makarwal group, Cherat group, Rawalpindi group and siwalik group consisting of sedimentary rocks, sandstone and shale (Geological Survey of Pakistan, 2007). The red rocks and sandstone exposed near GT road towards Taxilla are 20 million years old. The study area is located in an active faulting and folding tectonic zone and experience frequent earthquakes (RDPI, 2013). Oil and gas reserves have been found near Gujar Khan and as a result Gujar Khan is developing towards a highly urbanized city and attracting many companies (Ministry of Petroleum and Natural Resources, 2013).

2.1.5 Hydrology

Jhelum River flows in the eastern part of study area through gujar khan, Kahuta, Kallar syedan and Kotli Sattian. Soan River originates from southeastern part of Margalla hills and flows through Potohar region and drains water in the simli reservoir. Another river that flows through this region is Korang River which originates from Murree catchment and drains in Soan River afterwards. There are two dams built in study area i.e. Rawal Dam constructed on Korang River and Simli Dam constructed on Soan River. Both of these reservoirs are fed through rain and snow melt from the upstream catchments and provide water for Rawalpindi and Islamabad cities. In addition, Nullah Lai has a stream network throughout Rawalpindi and Islamabad and plays an important role in the urban flooding and drainage. Small local streams and numerous channels also originate from Margalla and Murree hills and drain into Nullahs and Rivers (Shiekh *et al.*, 2007).

2.1.6 Flora and Fauna

The study area has a diverse flora and fauna with a rich forest cover at the north eastern part and many rare species of animals. Margalla Hill National Park (MHNP) located in Islamabad is one of the protected areas due to its bio-diversity. Fauna including Leopard, Wild boar, Rhesus monkey, foxes, barking deer, jackals, jungle cats, scaly ant-eater and Marten inhabit the Islamabad and coniferous forests of Murree (Khan, 2006). Daboia (Russels's viper) and Indian cobra are present among reptiles (Khan, 2006). Many species of fishes including *Labeo rohita, Barilius pakistanicus, Labeo dero, Puntius ticto* and carp fish are found in the Rawal and Simli lakes (Nazeer et al., 2016). A rare endemic rodent species named as Murree vole is also found in the area. Many threatened species of birds including Vultures, Pariah eagle, Black kite, Kalij pheasant, Cheer pheasant (Chakor) and winter waterfowls are found in the study area (Yousaf and Manzoor, 2014; Khan, 2006). Different species of plants and trees including strawberries, cherries, pines, raspberries, jasmine, olive and chestnut are found in the eastern part of study area i.e. Murree, Islamabad and Kotli Sattian (Hameed et al., 2012). In addition, local shrubs and grasses, trees of Saccharum bengalense (Kana), Dalbergia sissoo (Sheesham), Vachellia karoo (Kikar), Acacia modesta (Phulai), Pyrus pasha (Pear), Bauhinia variegate (Kachnar) and Cedrus deodara (Deodar) are also common (Ali and Malik, 2010). Pines trees are common in Murree tehsils (Khan, 2006).

2.2 Datasets Acquired

Satellite data acquired from USGS LPDAAC and climatic data acquired from PMD (Pakistan Metrological Department) were used in this study. Multi-temporal Landsat satellite data and daily climatic data were collected from 1993 till 2015. The path/row followed for L5 TM, L7 ETM+ and L8 OLI-TIRS was 150/36 and 150/37. Climatic parameters (minimum temperature, maximum temperature and rainfall) data were collected for the stations of Rawalpindi and Islamabad cities.

2.3 Data Analyses

Analyses were performed in a series of steps involving the preparation and processing of data with the help of different software viz., ArcMap 10.1, ERDAS Imagine 2014, ENVI 5.3, Google Earth and Microsoft Excel. Data preparation included pre-processing of satellite data in ERDAS Imagine 2014. The satellite images were subjected to image enhancement and conversion of DN values into reflectance. As the Landsat image comes in variety of raster bands, stacking was done to produce a single raster composite for further processing. After stacking, the next step was mosaicking of both tiles and finally subsetting was performed to extract the area of interest in order to reduce the spatial resolution. The thermal band of Landsat was also preprocessed and its resolution was re-sampled from 120 meters to 30 meters.

2.3.1 Supervised Classification

Recognition of entities and phenomenon on earth is the main focus of remote sensing and classification is the best fitted technique for this purpose (Kokalj and Ostir, 2007). After pre-processing, supervised classification was applied on the satellite image. Supervised classification is quantitative process which allots each pixel to an individual class. Four LULC classes were formed namely vegetation, open land, built up area and water features. The description of these classes is given in table 2.1. The initial and essential step of supervised classification is collection of training samples for each class into a signature file. After defining the LULC categories, 200-300 training samples were observed for each class. The objects were identified on the basis of their spectral signatures in different bands.

Every object on earth reflects and absorbs the solar energy and has typical behavior represented in each wavelength of the solar spectrum known as the spectral profile of the object. For instance, water reflects blue wavelength but absorbs the infrared energy thus creating a profile of reflectance and absorbance in different bands of the raster. The objects were placed in a specific class with best match and then classification process was executed. Maximum likelihood algorithm was used for generating the classified image of land use and land cover of the study area. Maximum likelihood algorithm places the pixels in the class of highest probability (Patil *et al.*, 2012). It is the most efficient and widely used method so far and has proven to deduce best results for analyzing the land dynamics. Ground truthing was done to classify the dubious areas by using data from Google Earth and existing maps of the study area. All the four images were classified using similar method to derive the final LULC change for the past 23 years. Finally area was calculated for each land cover class.

Table 2.1: Land cover and Land use Classes

S.No	Class name	Description
1.	Vegetation	Includes the forest cover, agricultural land, vegetation in parks and greenbelts
2.	Open Land	Includes the barren land, rocks, desertified land and fallow land.
3.	Built Up	Commercial buildings, residential blocks, roads, bridges and other infrastructure.
4.	Water	Rivers, lakes, dams, small streams and nullahs.

2.3.2 Accuracy Assessment

The final stage of supervised classification is the accuracy assessment of the produced output to evaluate over all accuracy and Kappa Co-efficient (Rawat and Kumar, 2015). The accuracy assessment was performed by generating the reference control points and verifying them from ground truth data from Google Earth. The accuracy of classification was generated in the form of error matrix which gave information about the samples that were classified incorrectly and gave the overall accuracy percentage. The incorrectly classified samples were then corrected by using the recode tool in ERDAS Imagine.

2.4 LST (Land surface Temperature) Retrieval

The land surface temperature is the temperature of earth's surface at a given time and depends on the quantity of vegetation and impervious surfaces that are present in the area (Sobrino et al., 2013). For urban climate studies, LST is directly involved and gives information about the thermal characteristics of different land cover classes because the heat trapped and emitted from the earth determines the weather patterns and climate (Mallick *et al.*, 2008). Prior to calculating LST, Digital number values of pixels have to be converted into spectral radiance because the Digital number value stores the radiance but gives no information itself (Shah and Ghauri, 2015). LST of the study area was calculated from the TIR (Thermal Infra Red) band of Landsat. The Planck's equation used for deriving LST (Artis and Camahan, 1982) is as follows:

$$St = \frac{T}{1} + \left(\lambda \times \frac{T}{\rho}\right) \ln \epsilon \text{.........Eq 1}$$

Where,

St is the Land Surface Temperature,

T is the brightness temperature,

λ is the wavelength of TIR band,

and ϵ is the land surface emissivity.

Whereas, ρ is equal to h/cσ, where h is the planck's constant, c is velocity of light and σ is the Stefan's constant. ρ = 0.01438 mK.

For brightness temperature (T), following equation was used:

$$T = \frac{K2}{\ln\left(\frac{K1}{L\lambda} + 1\right)} \text{ ....Eq II}$$

Where,

K_2 and K_1 are band-specific constants determined by the wavelength of sensor.

Table 2.2: Values of K_1 and K_2

Sensor	K_1 ($W\ m^{-2}\ sr^{-1}\ um^{-1}$)	K_2 (Kelvin)
L5-TM	666.09	1282.71
L7-ETM+	607.76	1260.56
L8-(OLI/TIRS) B10	774.89	1321.08
L8-(OLI/TIRS) B11	480.89	1201.14

L_λ is the surface radiance which was calculated by the following equation:

$$L\lambda = \left[\frac{Lmax - Lmin}{QCALmax - QCALmin}\right] \times (DN - QCALmin) + Lmin \text{ ....Eq III}$$

Where,

L_{max} and L_{min} are maximum and minimum radiations,

DN is the pixel value of DN,

and $QCAL_{max}$ and $QCAL_{min}$ are calibrated energies and have specified value.

After calculating the radiance and brightness temperature, Emissivity was calculated by using NDVI through equation mentioned below.

$$\epsilon = 0.004PV + 0.986 \text{..........Eq IV}$$

PV stands for the proportion of vegetation and was calculated as follows:

$$PV = \left[\frac{NDVI - NDVImin}{NDVImax - NDVImin}\right] 2 \text{..........Eq V}$$

Finally, LST was retrieved by using equation I and compared with ground station based temperature data to determine the accuracy.

2.5 NDVI

Normalized Difference Vegetation Index is the quantitative measure of distribution of vegetation in an area because dense vegetation strongly reflects near infrared. The greater the vegetated area, greater the emissivity and lesser the vegetated area, lesser the emissivity (Maimaitiyiming *et al.*, 2014). NDVI was derived through atmospherically corrected Landsat images through following equation (Dwivedi *et al.*, 2015):

$$NDVI = \frac{NIR\ Band - RedBand}{NIR\ Band\ + RedBand}$$

2.6 Overlay Analysis for UHI

Overlay analysis was performed to find out the final urban heat spots. Overlay combines the information from all input layers and produces a merged layer as an output with combined characteristics of all input layers (Zhang *et al.*, 2013). The reclassified raster layers (LST, LULC and NDVI) were combined on the basis of their attributes and final UHI maps were derived.

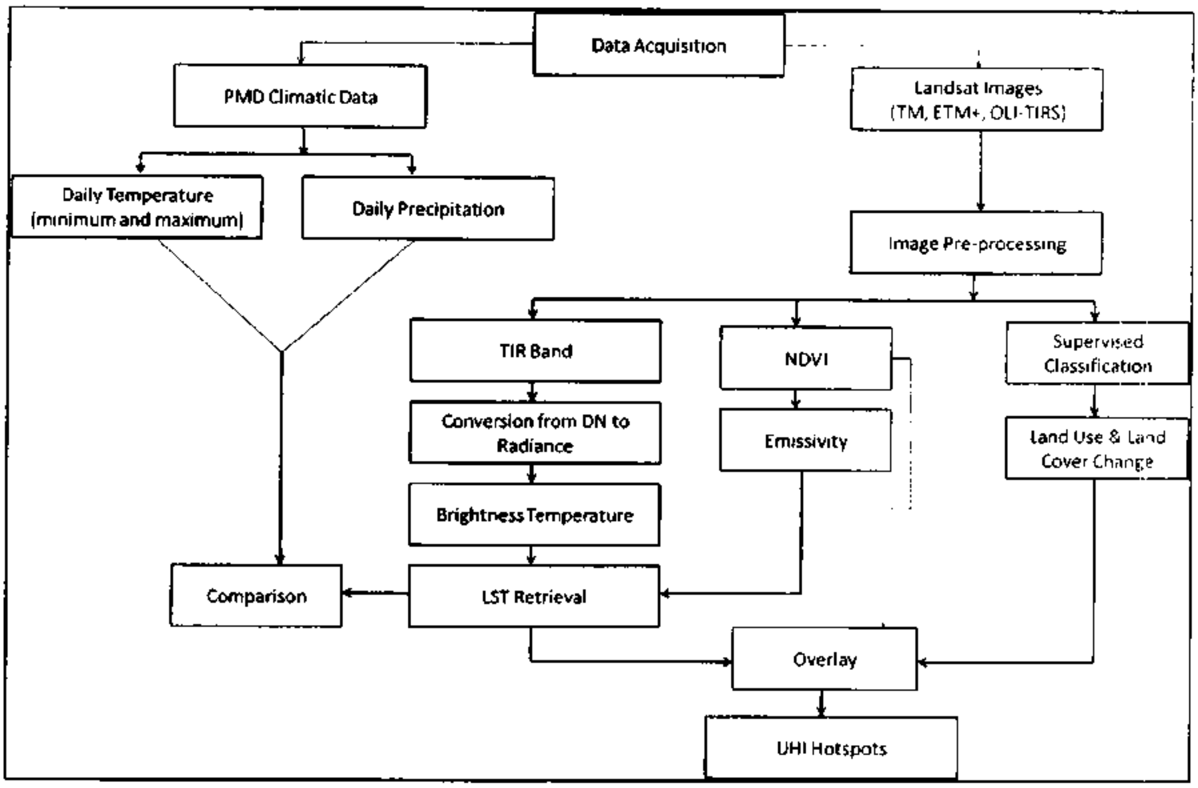

Figure 2.2: Flowchart of Methodology used for this Research

Chapter 3

Results and Discussion

3.0 Results and Discussion

This chapter features the results of data analysis that was employed to meet the objectives of this study. The findings for three objectives of this study viz., multi temporal land use land cover change mapping, multi temporal analysis of LST and the detection of urban heat hotspots are presented herewith.

3.1 Land Use and Land cover Change

The distribution of land use and land cover categories within the study area for the years 1993 to 2015 is presented in this section. Land use dynamics were estimated and compared for the years 1993, 2001, 2010 and 2015. The findings showed that over the past 22 years there has been a significant development and urbanization and clear reduction in forest cover. Figure 3.1(a) shows the LULC pattern of June 1993 and the percentages of each class within the study area. The vegetation of the area showed 57.47% cover with open land coverage of 37.62%. It was the time before construction of the mega projects in Islamabad city. Also in Rawalpindi. there was less agglomeration and built up of avenues and transformation of natural cover into built up areas. The percentage of built up area was very low at that time i.e. 3.69% due to low population density and the vegetation was abundant covering more than half of the total area as the developmental activities were not so vigorous.

Over a period of decade, a comparison has been presented for year 2001 in Figure 3.1b. The vegetation cover decreased from 57.47% to 52.97% mainly due to land clearing for construction which is obvious from increase in built up area up to 7.09% which is almost double then it was in 1993. Increase in the open land has been observed to 38.79% as a result of vegetation loss and harvesting season of crops. The vegetation thinning has resulted due to the expansion of roads in already urbanized area. Impervious area has increased due to construction of new housing colonies along highways and expansion of city areas towards suburbs to meet the increasing population demands. The water bodies showed decrease of 1.13% because urbanization and warming also affects water levels (LeBlanc et al., 1997).

The LULC statistics show that class distribution has changed dramatically from 2001 to 2010 (Figure 3.1c) because the urbanization process took place at a very rapid pace between these years. During this decade, avenues were built up in the federal city of Islamabad along with land clearing of Margalla hills for the construction of Monal resort. The vegetation cover has dropped to less than half i.e. 26.39%. The total percentage of built up area is 11.04% and mainly the areas of Rawalpindi, Islamabad, Gujar khan, Taxilla and Kallar Syedan have undergone major development while Murree and Kotli Sattian have also experienced urbanization due to construction of tourist resorts and new housing schemes. Tehsil Gujar khan has turned into major commercial and industrial hub because of the discovery of oil and gas reserves in 2002 whereas, the rest of areas have experienced innumerous construction of housing centers which expand into new phases each year. The vegetation level has drastically fallen and the open land has increased up to 61.75% because the construction of a large number of housing estates, commercial plazas, malls and other infrastructure resulted in clearing of land mainly vegetated land. Deforestation to produce timber for construction and industrial purposes has also contributed to the reduction of vegetative land. The areas under incomplete construction activities and digging also give the signature of soil or open land. Before June, the harvesting season of main crops of Rawalpindi district also leaves the land vacant and open. Moreover, in year 2010 water bodies have dried up as a result of hot weather and constituted only 0.8% of the total area. At that time population of the area experienced water shortage problems as well. The water demands of the increased population could not be met up by decreasing water reservoirs. This is attributed mainly to change in weather conditions i.e. change in temperature regime.

Figure 3.1d depicts the recent LULC setting of the June 2015 where it can be observed that built up area has increased up to almost 20% of the total area because large scale development has led to the construction of significant infrastructure, houses, commercial buildings and offices. The vegetation cover has improved to 30.4% because of the rehabilitation activities by the government to restore the overall forest cover so the ratio of open and desertified land has also decreased to 49%. The area covered by water is 0.72 because the month of June is hottest and causes the water level extent to decrease.

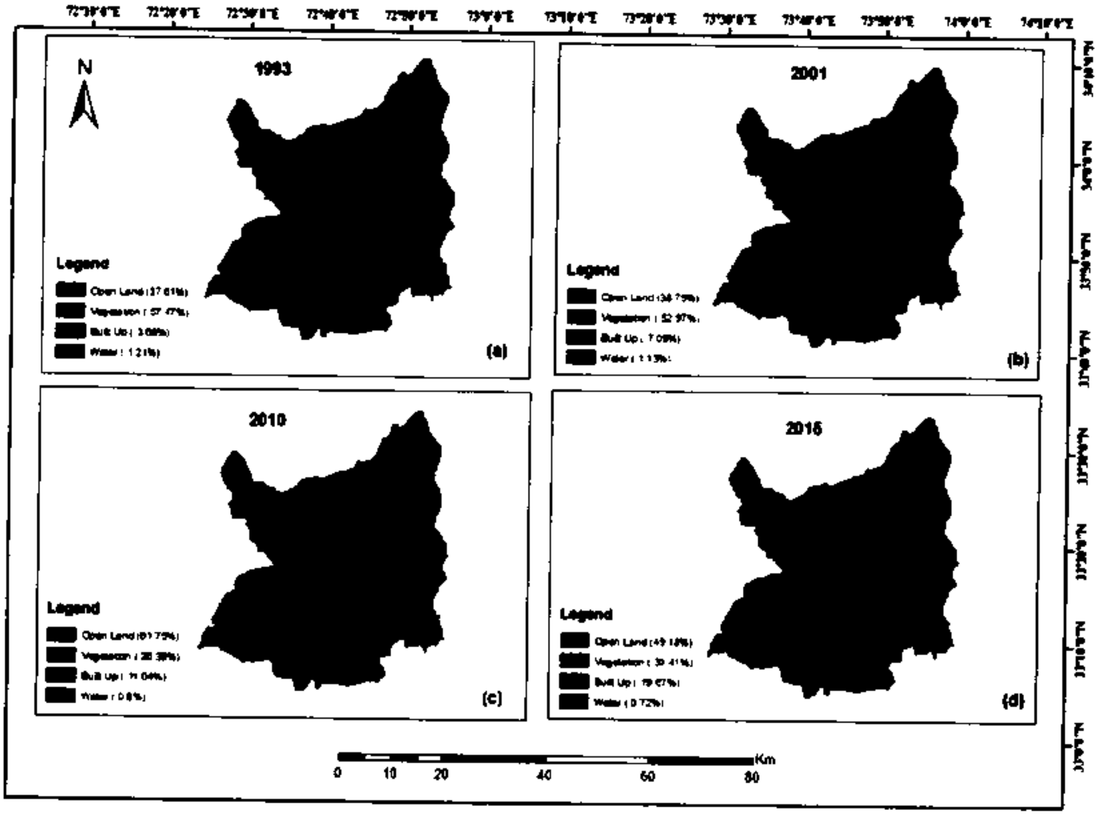

Figure 3.1: Map showing LULC of Rawalpindi and Islamabad districts 1993-2015 (a) LULC pattern 1993 (b) LULC pattern 2001 (c) LULC pattern 2010 (d) LULC pattern 2015

The overall accuracy of all classified images is above 80% and Kappa Co-efficient is 0.81. The accuracy assessment was done using the existing classified images and scanned maps of the study area and geo-referenced data from Google Earth. Figure 3.2 shows the combined statistics for the LULC change for all the considered instances. Moreover, total area for each class was calculated and presented in table 3.1.

Table 3.1: Area of LULC Classes (1993-2015)

Year	Area (Sq Km)			
	Open Land	Vegetation	Built Up	Water
1993	2300.05	3514.52	225.7	74.11
2001	2371.92	3238.77	433.75	69.54
2010	3775.83	1613.55	675.27	49.47
2015	3007.16	1859.74	1202.71	44.37

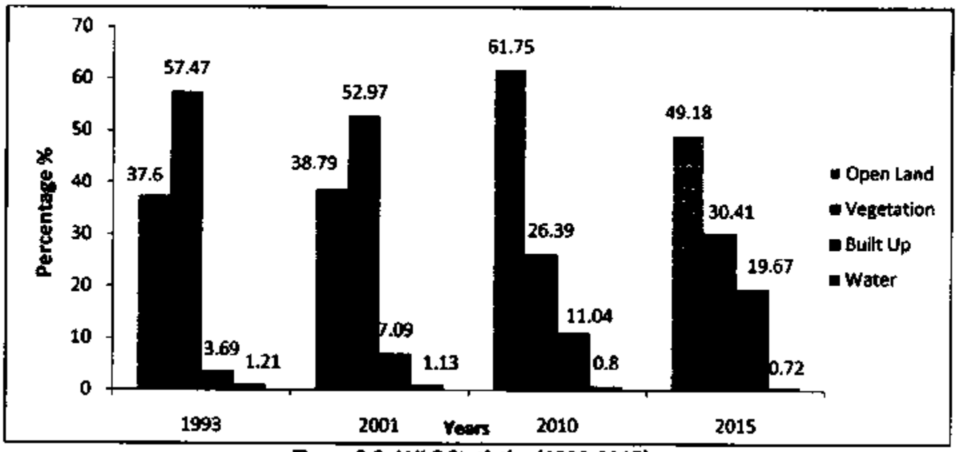

Figure 3.2: LULC Statistics (1993-2015)

The findings depict that land use trends have changed at a significant level during 1993-2015. A clear increase in impervious surfaces and major decline in the green cover within study area has been observed. Over the period of two decades, urban expansion has occurred to an enormous level throughout the area most specifically the areas which were already highly urbanized and populated.

3.2 Land Surface Temperature (LST)

There is a close relation between land cover and temperature because transformation of natural landscape into anthropogenic land use and land cover causes the earth's physical properties to change and this change affects LST (Lo and Quattrochi, 2003). Albedo of impervious surfaces is very low while the albedo of natural surfaces such as grass and water is high. Construction of houses, roads and other buildings require removal of forests and grasslands. Impervious surfaces such as roads, buildings and other infrastructure absorb heat and retain high temperature even after the sunset. A lot of transporting vehicles are functional in the cities which contribute to the high temperature by releasing GHG's and smoke. Contrary, rural areas cool down rapidly as there is less infrastructure and dense vegetation which does not store heat and thus keeps the temperature low as compared to the urbanized areas. The main reason for high temperature in big cities is human activities and anthropogenic land use land cover which changes the landscape and land surface properties.

For each year considered, LST was calculated to assess the temperature dynamics of study area. This section includes the results of LST for years 1993, 2001, 2010 and 2015. The LST of the study area for all the respective years is shown in figure 3.3. The minimum value calculated for LST in 1993 is 14.3°C while the maximum is 40.2°C. In 1993, the cities were not so much crowded and development process was very slow. Besides, the forest cover was sufficient and intact so, the areas experiencing maximum temperatures were very less while most of the area had medium and lesser temperature as shown in figure 3.3a. The change in LULC particularly reduction of forest cover and doubling of the percentage of urban area has resulted in rise of temperature in year 2001 which is shown in LST pattern (Figure 3.3b). The minimum temperature was raised to 16.4°C while maximum value increased upto 45.7°C.

Later after another decade in 2010, the minimum and maximum temperatures reached upto 15.8°C and 44.3°C respectively. The temperature profile was stable in comparison to year 2001 but is slowly and gradually increasing till 2010. Satellite data statistics shows an increase in minimum and maximum temperature in Islamabad between 2001 and 2010 which can be correlated to avenues construction in that time frame in Islamabad city. The LST of years 2001 and 2010 got high due to the intense climatic and metrological conditions which also influence the daily LST (Zhang et al., 2014).

A bit stable temperature trend is seen in later years in the study area although land clearing is at its peak for construction and developmental projects. The minimum land surface temperature value for the year 2015 is 15.4°C and maximum is 41.8°C. LULC of year 2015 shows an increase in vegetation cover due to plantation and aforestation activities. The distribution of areas having maximum temperature has also increased throughout the study area both in 2010 and 2015 due to increase in impervious surfaces.

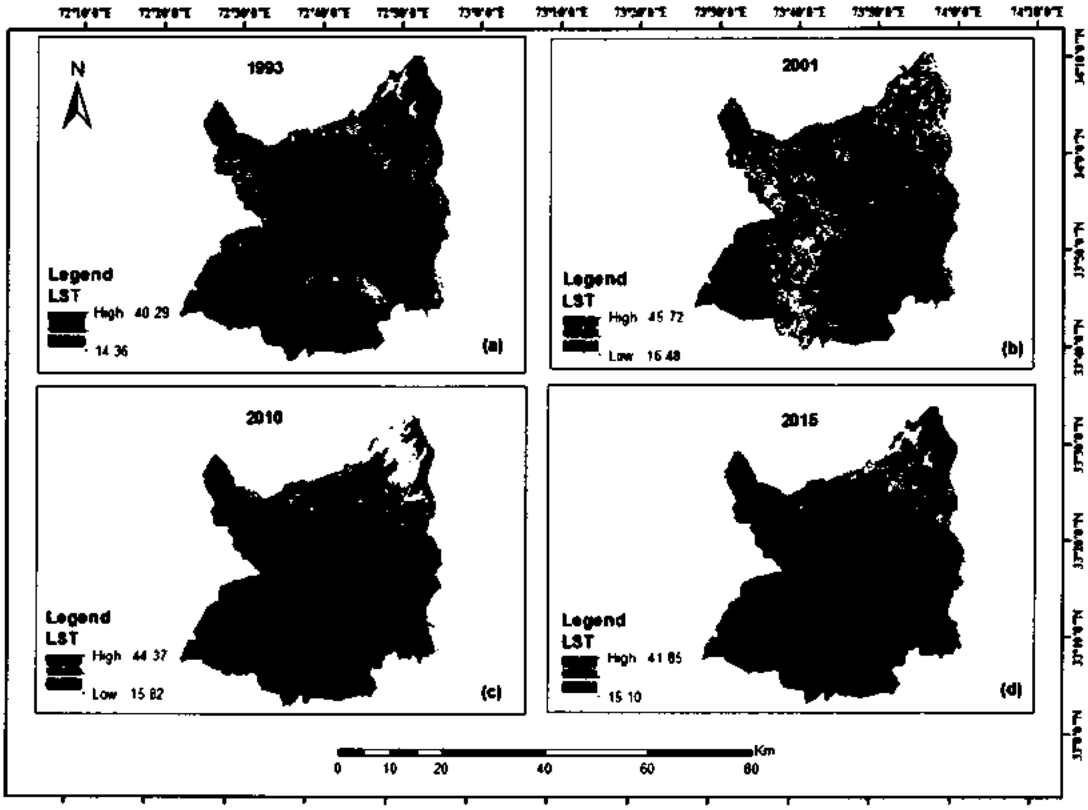

Figure 3.3: Land Surface Temperature profile from 1993-2015 (a) LST pattern 1993 (b) LST pattern 2001 (c) LST pattern 2010 (d) LST pattern 2015

Daily temperature and rainfall data of available station (Rawalpindi Tehsil and Islamabad District) collected from Pakistan Metrological Department (PMD) was also analyzed. Rainfall for all the considered instances was 0mm whereas the temperature has been shown in figure 3.4.

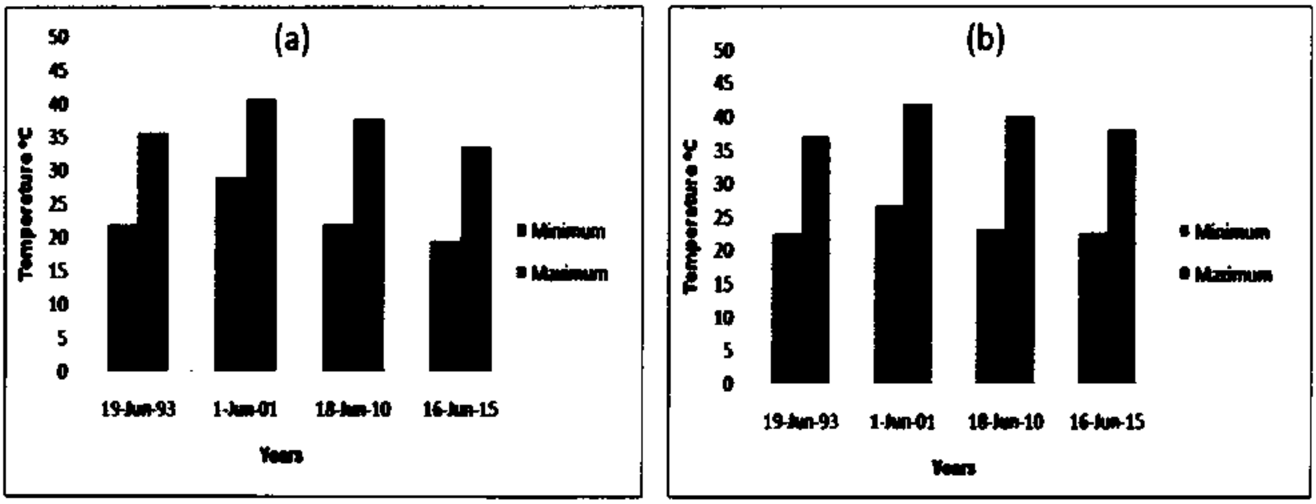

Figure 3.4: Graph showing Minimum and Maximum Temperature recorded by PMD for (a) Rawalpindi Tehsil and (b) Islamabad District

Because weather and climatic changes becomes obvious in minimum of 30 years time frame (Huber and Gulledge, 2011) therefore if we conclude from 1993 and 2015, changes are obvious, but for short time instances considered in between, changes are not obvious as the instance may be affected by the metrological conditions of that time or an extreme weather event.

3.3 Urban Heat Island

Urban heat islands are zones with modified and complicated climate which is formed usually in densely populated and urbanized areas when the concrete, steel, glass and other impervious surfaces absorb solar radiation and trap it raising the temperature of that particular area (Barnes et al., 2001). The temperature of UHI prone areas is several degrees higher than the rural areas adjacent to them (Devi, 2006). In addition to the absorption of solar heat by impervious surfaces, artificial heat through vehicular emissions and industrial production also exacerbate UHI effect. Lack of ventilation and air movements due to tight urban geometry both horizontally and vertically intensifies this effect (Liu and Liu, 2012). The temporal distribution of urban heat islands throughout the study area is shown in figure 3.5. The findings show that the formation of urban heat islands is mainly in areas with high built up and opens land as both of these are impervious surfaces having greater capacity of heat absorbance and storage.

A clear climatic modification can be observed in the study area from 1993 to 2015. The findings reveal that UHI intensity is high in areas with urban and open land whereas low to medium in zones with sufficient vegetation and less built up. The difference in temperature is due to the fact that urban sprawl towards the non-urbanized areas has caused the ratio of impervious surfaces to increase and trigger the formation of UHI phenomenon. The temperature for open land is higher as it has more surface area, sand content and capacity to absorb heat while that of built up is slightly lower (Shah and Ghauri, 2015). The UHI prone areas were divided into five categories i.e. very low, low, medium, high and very high on the basis of difference in land surface temperature between them.

The "Very low", "Low", "Medium", "High" and "Very high" temperature areas have LST difference of 1-3°C, 3-6°C, 6-8°C, 8-12°C and 12-15°C respectively from their surroundings and less urbanized areas. The resultant UHI maps for year 1993 clearly depicts a smaller portion of area with high UHI intensity (Figure 3.5a) but increased distribution of "very high" temperature zone is visible from 2001-2015 (Figure 3.5).

In 1993, the extent of UHI effect was very less and confined to Rawalpindi tehsil of the study area as shown in figure 3.5a. The built up area was low in 1993 and a dense vegetation cover was present which allowed less radiation to be absorbed in the absence of impervious surfaces. A decade later in year 2001, built up area increased in Islamabad and Rawalpindi cities due to the construction and expansion activities therefore the distribution of high UHI zone also increased. It was observed that the temperature extent was high for built up and open land due to clearing of vegetation in comparison to vegetated and green areas. This is in relevance to LULC change results for these years (See Figure 3.1 for details) Islamabad district and Taxilla tehsil which had low UHI extent in 1993 transformed into "very high" whereas in year 2001 many previously low temperature areas turned into "medium" category as compared to their adjacent areas (Figure 3.5b).

Later up to year 2010, UHI zone with "very high" effect can be seen widely distributed throughout the study area. Tehsils of Gujar Khan, Kahuta and Kallar Syedan which were relatively cooler in the previous years have been transformed into "high" and "very high" category as shown in Figure 3.5c. The vacant land was in very high percentage while the vegetation was lowest during the year 2010 (Figure 3.1c). There was not massive development and construction in Murree and Kotli Sattian but recently these areas are also being urbanized because of construction of tourist attraction and recreational facilitates such as amusement parks, hotels, apartments etc. The results showed that the temperature in vegetated areas and water bodies is low as compared to built up areas and vacant land and falls in the low category even if the surrounding temperature is high. Though plantation projects by federal and provincial authorities have contributes to the increase of vegetation cover from 26.39% to 30.4% in 2015 (See Figure 3.1 for details), the UHI still seems to expand its extent as the construction and development activities have no limit to them. The "very high" zone has dominated the major part of the study area in year 2015 as shown in Figure 3.5d. It is concluded that from 1993 to 2015, UHI intensity and distribution has increased dramatically in districts of Rawalpindi and Islamabad. Areas become hotter as robust urban expansion is at its peak.

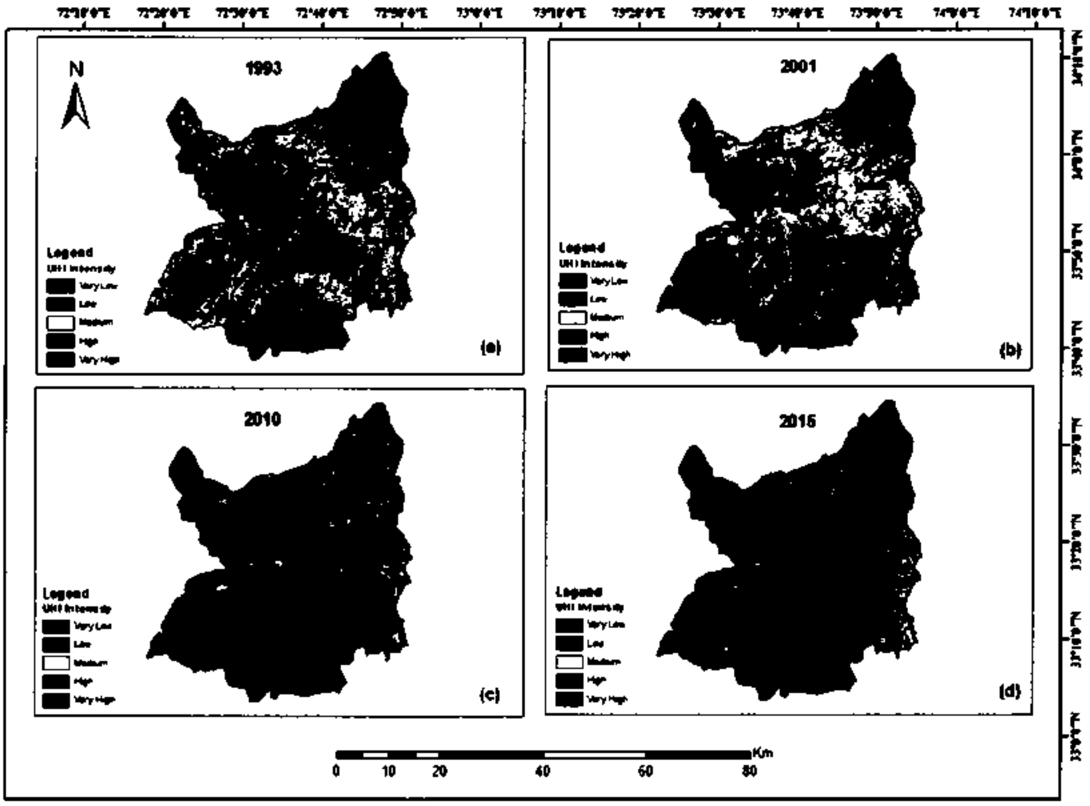

Figure 3.5: Urban Heat Island Map (a) UHI pattern 1993 (b) UHI pattern 2001 (c) UHI pattern 2010 (d) UHI pattern 2015

References

References

Ali, S. M., & Malik, R. N. (2010). Spatial patterns of vegetation with underlying soil properties prevailing along drain side Areas in Islamabad city. Pak. J. Bot, 42(4), 2397-2410.

Aniello, C., Morgan, K., Busbey, A., & Newland, L. (1995). Mapping micro-urban heat islands using Landsat TM and a GIS. *Computers & Geosciences, 21*(8), 965-969.

Artis, D. A., & Carnahan, W. H. (1982). Survey of emissivity variability in thermography of urban areas *Remote Sensing of Environment, 12*(4), 313-329.

Balogun, I. A., Adeyewa, D. Z., Balogun, A. A., & Morakinyo, T. E. (2011). Analysis of urban expansion and land use changes in Akure, Nigeria, using remote sensing and geographic information system (GIS) techniques. *Journal of Geography and Regional Planning, 4*(9), 533.

Bass, B., Krayenhoff, S., Martilli, A., & Stull, R. (2002). Mitigating the urban heat island with green roof infrastructure. *Urban Heat Island Summit: Toronto.*

Brazel, A., Selover, N., Vose, R., & Heisler, G. (2000). The tale of two climates Baltimore and Phoenix urban LTER sites. *Climate Research, 15*(2), 123-135.

Changnon, S. A., Kunkel, K. E., & Reinke, B. C. (1996). Impacts and responses to the 1995 heat wave: A call to action. *Bulletin of the American Meteorological society, 77*(7), 1497-1506

Coseo, P., & Larsen, L. (2014). How factors of land use/land cover, building configuration, and adjacent heat sources and sinks explain Urban Heat Islands in Chicago. *Landscape and Urban Planning, 125*, 117-129.

Devi, S. S. (2006, January). Urban heat islands and environmental impact. In *86th AMS annual meeting*

Dihkan, M., Karsli, F., Guneroglu, A., & Guneroglu, N. (2015). Evaluation of surface urban heat island (SUHI) effect on coastal zone: The case of Istanbul Megacity. *Ocean & Coastal Management.*

Dwivedi, A., Khire, M. V., & Mohan, B. K. (2015). Estimation of Land Surface Temperature to Study Urban Heat Island Effect in Mumbai Using Landsat ETM+ Image.

Elaalem, M. M., Ezlit, Y. D., Elfghi, A., & Abushnaf, F. (2013). Performance of Supervised Classification for Mapping Land Cover and Land Use in Jeffara Plain of Libya. In *International Conference on Food and Agricultural Sciences* (Vol. 55).

Eumorfopoulou, E. A., & Kontoleon, K. J. (2009). Experimental approach to the contribution of plant-covered walls to the thermal behaviour of building envelopes. *Building and Environment, 44*(5), 1024-1038.

Gago, E. J., Roldan, J., Pacheco-Torres, R., & Ordóñez, J. (2013). The city and urban heat islands: A review of strategies to mitigate adverse effects. *Renewable and Sustainable Energy Reviews, 25*, 749-758.

Gartland, L. M. (2012). *Heat islands: understanding and mitigating heat in urban areas*. Routledge.

Gusso, A., Cafruni, C., Bordin, F., Veronez, M. R., Lenz, L., & Crija, S. (2015). Multi-Temporal Patterns of Urban Heat Island as Response to Economic Growth Management. *Sustainability*, 7(3), 3129-3145

Hamdi, R. (2010). Estimating urban heat island effects on the temperature series of Uccle (Brussels, Belgium) using remote sensing data and a land surface scheme. *Remote Sensing, 2*(12), 2773-2784.

Hameed, M., Nawaz, T., Ashraf, M., Ahmad, F., Ahmad, K. S., Ahmad, M. S. A., & Ahmad, I. (2012). Floral biodiversity and conservation status of the Himalayan foothill region, Punjab, Pak. J. Bot, 44, 143-149.

Hanqiu, X., & Benqing, C. (2004). Remote sensing of the urban heat island and its changes in Xiamen City of SE China. *Journal of Environmental Sciences, 16*(2), 276-281.

Huang, W., Zeng, Y., & Li, S. (2015). An analysis of urban expansion and its associated thermal characteristics using Landsat imagery. *Geocarto International, 30*(1), 93-103.

Imhoff, M. L., Zhang, P., Wolfe, R. E., & Bounoua, L. (2010). Remote sensing of the urban heat island effect across biomes in the continental USA. *Remote Sensing of Environment, 114*(3), 504-513.

Kandel, H., Melesse, A., & Whitman, D. (2016). An analysis on the urban heat island effect using radiosonde profiles and Landsat imagery with ground meteorological data in South Florida. *International Journal of Remote Sensing, 37*(10), 2313-2337.

Khan, H. (2006). Willingness to pay for margalla hills national park: evidence from the travel cost method. The Lahore Journal of Economics, 11(2), 43-70.

Kim, Y. H., & Baik, J. J. (2005). Spatial and temporal structure of the urban heat island in Seoul. *Journal of Applied Meteorology, 44*(5), 591-605.

Knowlton, K., Rotkin-Ellman, M., King, G., Margolis, H. G., Smith, D., Solomon, G., & English, P. (2009). The 2006 California heat wave: impacts on hospitalizations and emergency department visits. Environmental health perspectives, 117(1), 61.

Kokalj, Z., & Ostir, K. (2007). Land cover mapping using Landsat satellite image classification in the Classical Karst-Kras region. *Acta carsol, 36*(3), 433-440.

Kumar, K. S., Bhaskar, P. U., & Padmakumari, K. (2012). Estimation of land surface temperature to study urban heat island effect using LANDSAT ETM+ image. *International journal of Engineering Science and technology*, *4*(2), 771-778.

Li, D., Sun, T., Liu, M., Yang, L., Wang, L., & Gao, Z. (2015). Contrasting responses of urban and rural surface energy budgets to heat waves explain synergies between urban heat islands and heat waves. *Environmental Research Letters*, *10*(5), 054009.

Liu, H., & Liu, Q. (2012). The Urban Heat Islands Analysis: Factors of Building Surface, Green Area and Lighting

Liu, L., & Zhang, Y. (2011). Urban heat island analysis using the Landsat TM data and ASTER data: A case study in Hong Kong. *Remote Sensing*, *3*(7), 1535-1552.

Lo, C. P., & Quattrochi, D. A. (2003). Land-Use and land-cover change, urban heat island phenomenon, and health implications. *Photogrammetric Engineering & Remote Sensing*, *69*(9), 1053-1063.

Maimaitiyiming, M., Ghulam, A., Tiyip, T., Pla, F., Latorre-Carmona, P., Halik, U. & Caetano, M. (2014). Effects of green space spatial pattern on land surface temperature: Implications for sustainable urban planning and climate change adaptation. *ISPRS Journal of Photogrammetry and Remote Sensing*, *89*, 59-66.

Mallick, J., Kant, Y., & Bharath, B. D. (2008). Estimation of land surface temperature over Delhi using Landsat-7 ETM+. *J Indian Geophys Union*,*12*(3), 131-140.

Memon, R. A., Leung, D. Y., & Liu, C. H. (2009). An investigation of urban heat island intensity (UHII) as an indicator of urban heating. *Atmospheric Research*, *94*(3), 491-500.

Mirzaei, P. A. (2015). Recent challenges in modeling of urban heat island. *Sustainable Cities and Society*, *19*, 200-206.

More, R., Kale, N., Kataria, G., Rane, R. A., & Deshpande, S. (2015). Study of the Different Approaches used to Estimate the Urban Heat Island Effect in India. *Int J of Multidisciplinary and Scientific Emerging Research*, *4*(2).

Munier, K., & Burger, H. (2001). Analysis of land use data and surface temperatures derived from satellite data for the area of Berlin. *Remote sensing of urban areas Fernerkundung in urbanen Raaumen Regensburg ISBN*, 3-88246.

Nazeer, S., Hashmi, M. Z., & Malik, R. N. (2016). Spatial and seasonal dynamics of fish assemblage along river Soan, Pakistan and its relationship with environmental conditions. *Ecological Indicators*, 69, 780-791

Patil, M. B., Desai, C. G., & Umrikar, B. N. (2012). Image classification tool for land use/land cover analysis: A comparative study of maximum likelihood and minimum distance method. *International Journal of Geology Earth and Environmental Sciences*, *2*(3), 189-196.

Pena, M. A. (2008). Relationships between remotely sensed surface parameters associated with the urban heat sink formation in Santiago, Chile. *International Journal of Remote Sensing*, *29*(15), 4385-4404.

Quan, J., Chen, Y., Zhan, W., Wang, J., Voogt, J., & Wang, M. (2014). Multi-temporal trajectory of the urban heat island centroid in Beijing, China based on a Gaussian volume model. *Remote Sensing of Environment*, *149*, 33-46.

Rawat, J. S., & Kumar, M. (2015). Monitoring land use/cover change using remote sensing and GIS techniques: A case study of Hawalbagh block, district Almora, Uttarakhand, India. *The Egyptian Journal of Remote Sensing and Space Science*, *18*(1), 77-84.

RDPI. (2013). Rawalpindi and Islamabad: Multi Hazard Risk Mapping, Islamabad.

Sajjad, S. H., Blond, N., Batool, R., Shirazi, S. A., Shakrullah, K., & Bhalli, M. N. (2015). Study of Urban Heat Island of Karachi by Using Finite Volume Mesoscale Model. *Journal of Basic & Applied Sciences*, *11*, 101

Salim, A., Ahmed, A., Ashraf, N., & Ashar, M. (2015). Deadly Heat Wave in Karachi, July 2015: Negligence or Mismanagement? The international journal of occupational and environmental medicine, 6(4 October), 678-249.

Schwarz, N., Schlink, U., Franck, U., & Großmann, K. (2012). Relationship of land surface and air temperatures and its implications for quantifying urban heat island indicators: an application for the city of Leipzig (Germany). *Ecological Indicators*, *18*, 693-704.

Seinfeld, J. H., & Pandis, S. N. (2016). Atmospheric chemistry and physics: from air pollution to climate change. John Wiley & Sons.

Shah, B., & Ghauri, B. (2015). Mapping Urban Heat Island Effect in Comparison with the Land Use, Land Cover of Lahore District. *Pakistan Journal of Meteorology Vol*, *11*(22).

Shah, B., & Ghauri, B. (2015). Mapping Urban Heat Island Effect in Comparison with the Land Use, Land Cover of Lahore District. *Pakistan Journal of Meteorology Vol*, *11*(22).

Sheikh, I. M., Pasha, M. K., Williams, V. S., Raza, S. Q., & Khan, K. S. A. (2007). Environmental geology of the Islamabad-Rawalpindi area, northern Pakistan. *Regional Studies of the Potwar Plateau Area, Northern Pakistan. US Geological Survey, Reston*, G1-G28.

Sheng, L., Lu, D., & Huang, J. (2015). Impacts of land-cover types on an urban heat island in Hangzhou, China. *International Journal of Remote Sensing*, *36*(6), 1584-1603.

Shudo, H., Sugiyama, J., Yokoo, N., & Oka, T. (1997). A study on temperature distribution influenced by various land uses. *Energy and buildings*, *26*(2), 199-205.

Sidiqui, P., Huete, A., & Devadas, R. (2016). Spatio-temporal mapping and monitoring of Urban Heat Island patterns over Sydney, Australia using MODIS and Landsat-8. In *Earth Observation and Remote Sensing Applications (EORSA), 2016 4th International Workshop on* (pp. 217-221). IEEE.

Sobrino, J. A., R. O. Carrióa, G. Sòriaa , J. C. Jiménez-Muñoza , B. Francha , V. Hidalgoa , C. Mattara , Y. Juliena , J. Cuencaa, M. Romagueraa , J. A. Gómezb , E. Miguelb , R. Bianchic, and M. Paganinic. (2013). Evaluation of the surface urban heat island effect in the city of Madrid by thermal remote sensing. Intern. J. Remote Sens. 34, 3177–3192.

Stathopoulou, M., & Cartalis, C. (2007). Daytime urban heat islands from Landsat ETM+ and Corine land cover data: An application to major cities in Greece. *Solar Energy, 81*(3), 358-368.

Su, W., Gu, C., & Yang, G. (2010). Assessing the impact of land use/land cover on urban heat island pattern in Nanjing City, China. *Journal of Urban Planning and Development, 136*(4), 365-372.

UDESA, World Population Prospects: The 2010 Revision, Highlights and Advance Tables: Working Paper No ES/P/WP. 220. New York: United Nations, Department of Economic and Social Affairs, Population Division 2011.

Un-Habitat. (2014). Climate Change Vulnerability Assessment Report.

United Nations. (2010). World urbanization prospects: The 2009 revision population database.

Upmanis, H. (1999). The influence of sky-view factor and land-use on city temperatures. *Influence of Parks on local climate Earth Sciences Centre, Goteborg University, Paper, 3,* 1-15.

Upmanis, H., Eliasson, I., & Lindqvist, S. (1998). The influence of green areas on nocturnal temperatures in a high latitude city (Göteborg, Sweden). *International journal of climatology, 18*(6), 681-700.

Voogt, J. A. (2007). How researchers measure urban heat islands. Washington: USEPA.

Weng, Q., Lu, D., & Schubring, J. (2004). Estimation of land surface temperature–vegetation abundance relationship for urban heat island studies. *Remote sensing of Environment, 89*(4), 467-483.

Wright, A. J., Young, A. N., & Natarajan, S. (2005). Dwelling temperatures and comfort during the August 2003 heat wave. *Building Services Engineering Research and Technology, 26*(4), 285-300.

Xian, G., & Crane, M. (2006). An analysis of urban thermal characteristics and associated land cover in Tampa Bay and Las Vegas using Landsat satellite data. *Remote Sensing of environment, 104*(2), 147-156.

Yousaf, N., & Manzoor, M. (2014). A Checklist of Birds of Prey of Rawalpindi, Islamabad and Adjacent Areas. Journal of Bioresource Management, 1(2), 3.

Yusuf, Y. A., Pradhan, B., & Idrees, M. O. (2014). Spatio-temporal assessment of urban heat island effects in Kuala Lumpur metropolitan city using Landsat images. *Journal of the Indian Society of Remote Sensing*, *42*(4), 829-837.

Zhang, H., Qi, Z. F., Ye, X. Y., Cai, Y. B., Ma, W. C., & Chen, M. N. (2013). Analysis of land use/land cover change, population shift, and their effects on spatiotemporal patterns of urban heat islands in metropolitan Shanghai, China. *Applied Geography*, *44*, 121-133.

Zhang, H., Qi, Z. F., Ye, X. Y., Cai, Y. B., Ma, W. C., & Chen, M. N. (2013). Analysis of land use/land cover change, population shift, and their effects on spatiotemporal patterns of urban heat islands in metropolitan Shanghai, China. *Applied Geography*, *44*, 121-133.

Zhao, L., Lee, X., Smith, R. B., & Oleson, K. (2014). Strong contributions of local background climate to urban heat islands. *Nature*, *511*(7508), 216-219.